

Supporting information:

Title: Poliovirus evolution toward independence from the phosphatidylinositol-4 kinase III β / oxysterol binding protein family I pathway

Author: Minetaro Arita and Joëlle Bigay

The number of pages: 18

The number of figures: 11

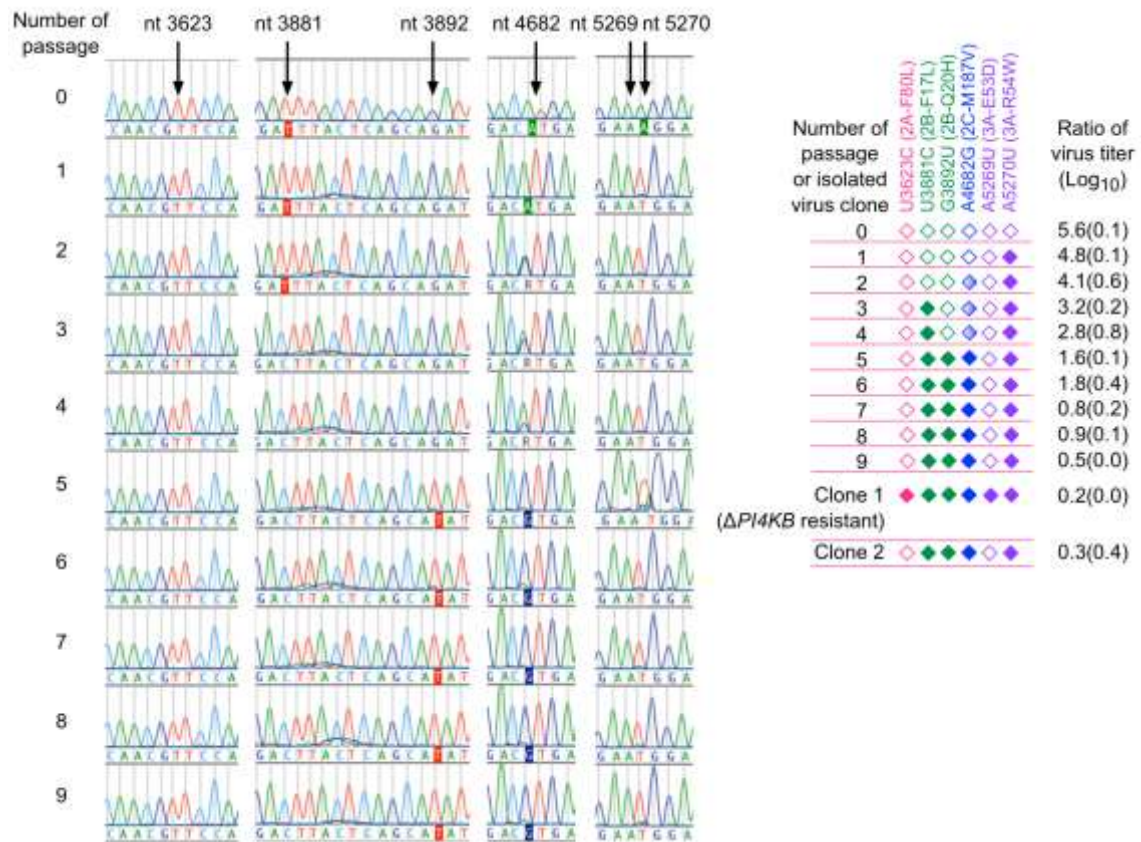


Figure S1. Evolutionary pathway of PV in RD(Δ PI4KB) cells.

Genomic sequences of PV (pooled populations or isolated clones) after indicated number of passage in RD(Δ PI4KB) cell. Filled diamonds represent nt mutation derived from PV1(Δ PI4KB resistant), and open diamonds represent nt of WT. Ratio of virus titer represents $\log_{10}(\text{CCID}_{50} \text{ in RD[WT]} \text{ cells} / \text{CCID}_{50} \text{ in RD}[\Delta\text{PI4KB}] \text{ cells})$. Standard deviation is shown in parentheses. $n = 2$.

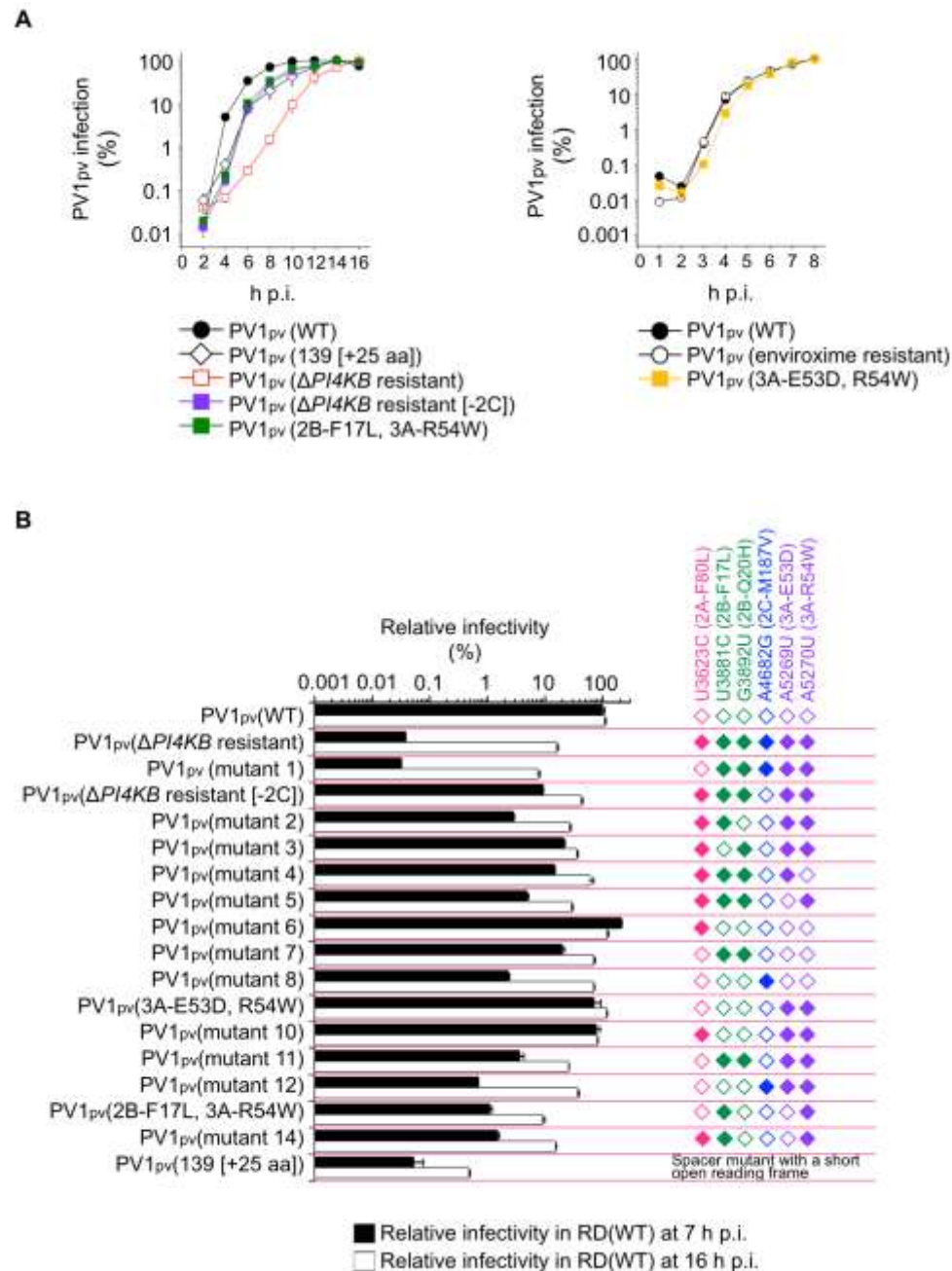


Figure S2. Replication kinetics of PV1_{pv} mutants.

(A) Luciferase activity in RD(WT) cells infected with PV1_{pv} mutants with the 2B/3A mutations or the 3A mutations were analyzed until 16 or 8 h p.i., respectively. Maximum signals observed during the infection are taken as 100%.

(B) Relative infectivity of PV1_{pv} mutants in RD(WT) cells. Filled diamonds represent nt mutation derived from PV1(Δ PI4KB resistant), and open diamonds represent nt of WT. PV1_{pv}(WT) infection at 7 h p.i. is taken as 100%.

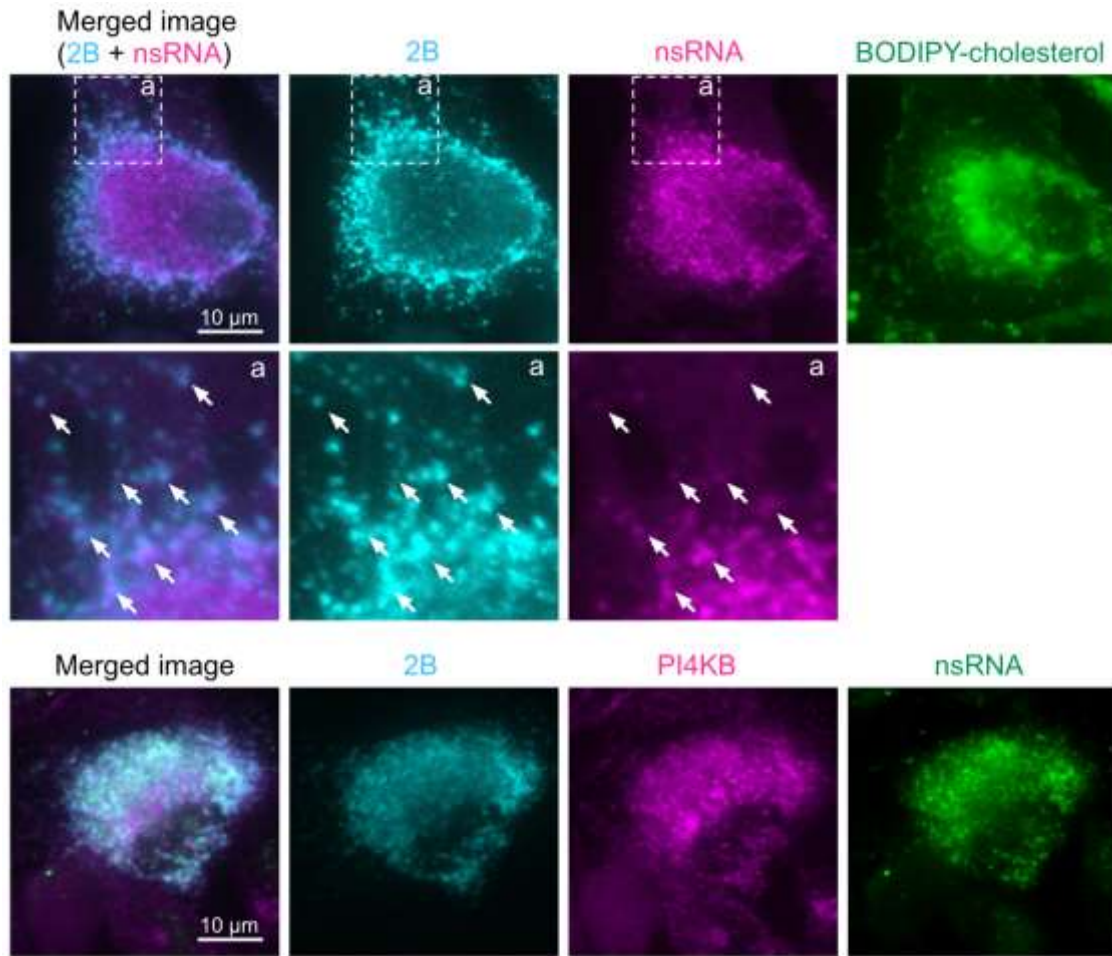


Figure S3. Localization of nascent viral RNA and 2B.

RD(WT) cells were infected with PV1_{pv}(WT) at an MOI of 2.5, and then fixed at 5 h p.i. for indirect immunofluorescence. The first row shows localization of 2B, nascent viral RNA (nsRNA), and BODIPY-cholesterol in the infected cells. The second row shows magnified views of the boxed areas in the first row. White arrows indicate some of the colocalized sites. The third row shows localization of 2B, PI4KB, and nsRNA in the infected cells.

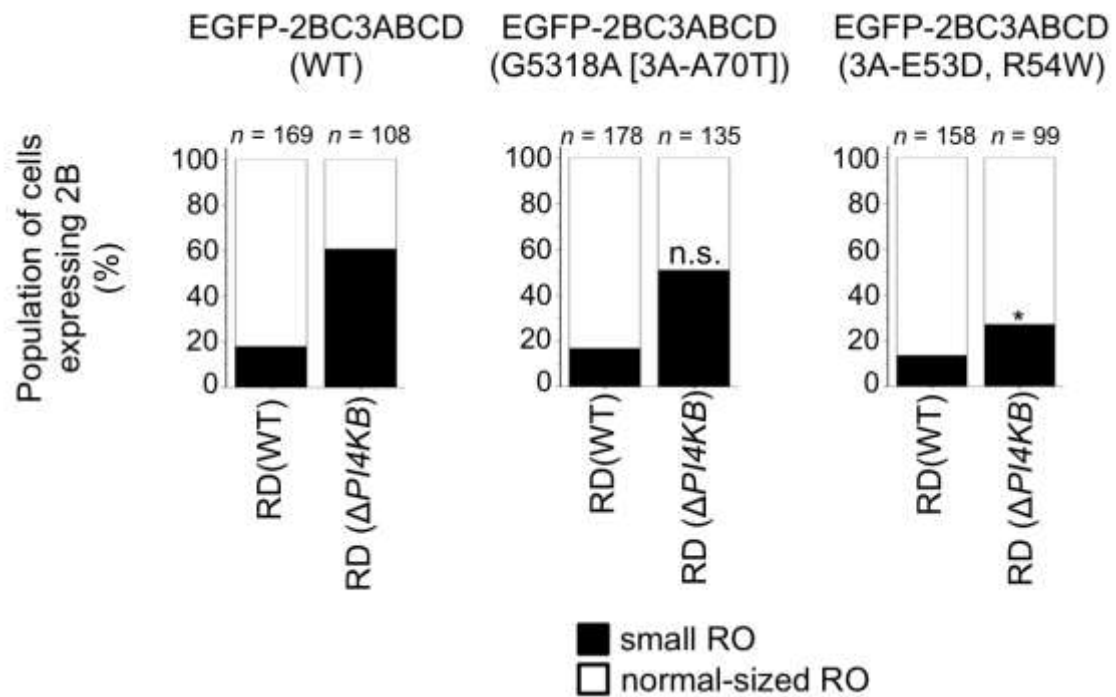


Figure S4. Effect of the 3A(G5318A[3A-A70T]) mutation on the RO development. N-terminally EGFP-fused PV polyprotein (EGFP-2BC3ABCD) with indicated mutations were overexpressed in RD(WT) and RD(Δ PI4KB) cells. Localization of 2B was analyzed as a marker of RO. Populations of cells with normal-sized or small RO are shown. n.s., not significant (vs. EGFP-2BC3ABCD[WT]).

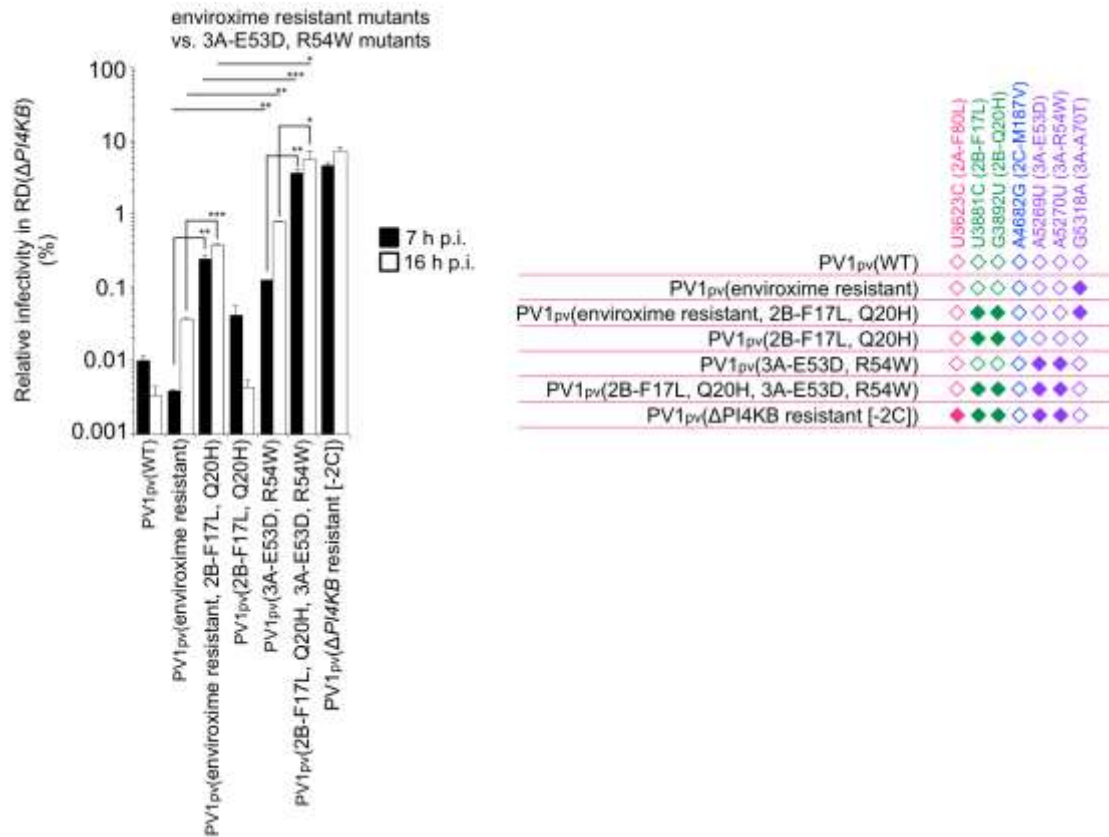


Figure S5. Specificity of the 3A mutations for the synthetic effect with the 2B mutations.

RD(WT) and RD(Δ PI4KB) cells were infected with PV1_{pv}, and then the luciferase activities were measured at 7 or 16 h p.i., respectively. PV1_{pv} infection in RD(WT) cells is taken as 100 %. Relative infectivity in RD(Δ PI4KB) cells is shown. Filled diamonds represent nt mutation derived from PV1(Δ PI4KB resistant), and open diamonds represent nt of WT. $n = 2$.

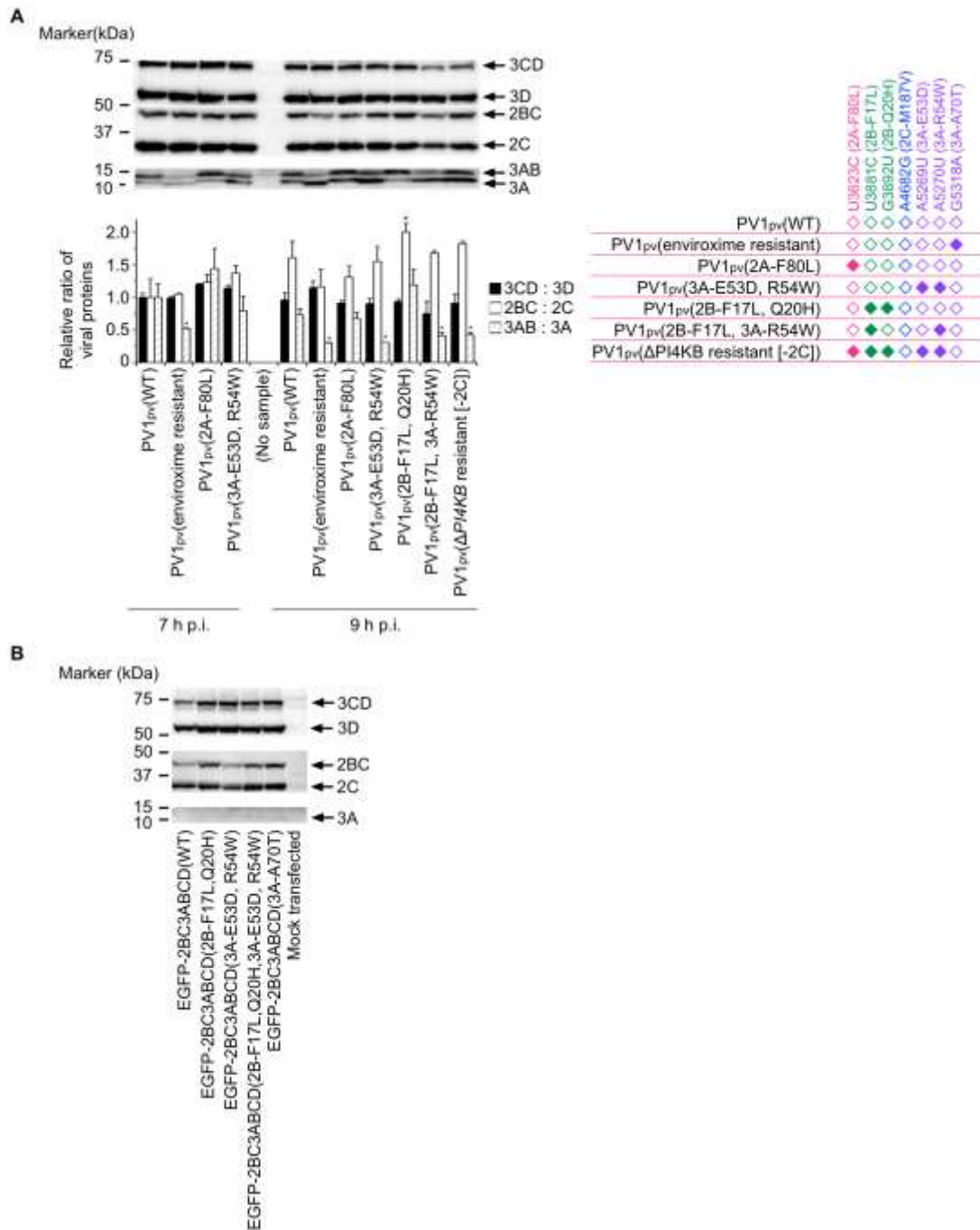


Figure S6. Effect of the 3A mutations on the processing of viral proteins.

(A) Western blot analysis of viral proteins in RD(WT) cells infected with PV1_{pv} mutants (at an MOI = 5.0, at 9 h p.i.). Relative ratios of each set of viral proteins are shown. The ratios in PV1_{pv}(WT) infection are taken as 1. Filled diamonds represent nt mutation derived from PV1(Δ PI4KB resistant), and open diamonds represent nt of WT. $n = 3$.

(B) Western blot analysis of viral proteins in HEK293 cells expressing EGFP-2BC3ABCD with indicated mutations at 24 h p.t.

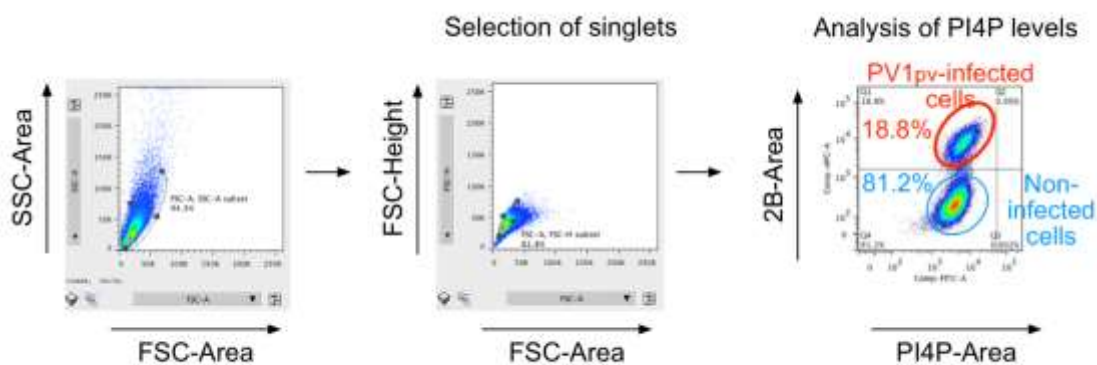


Figure S7. Gating strategy of flow cytometry.

Major population of the cells was selected by SSC-Area/FSC-Area window, and then singlets of the cells were selected in FSC-Height/FSC-Area window for quantification of the PI4P levels in the cells.

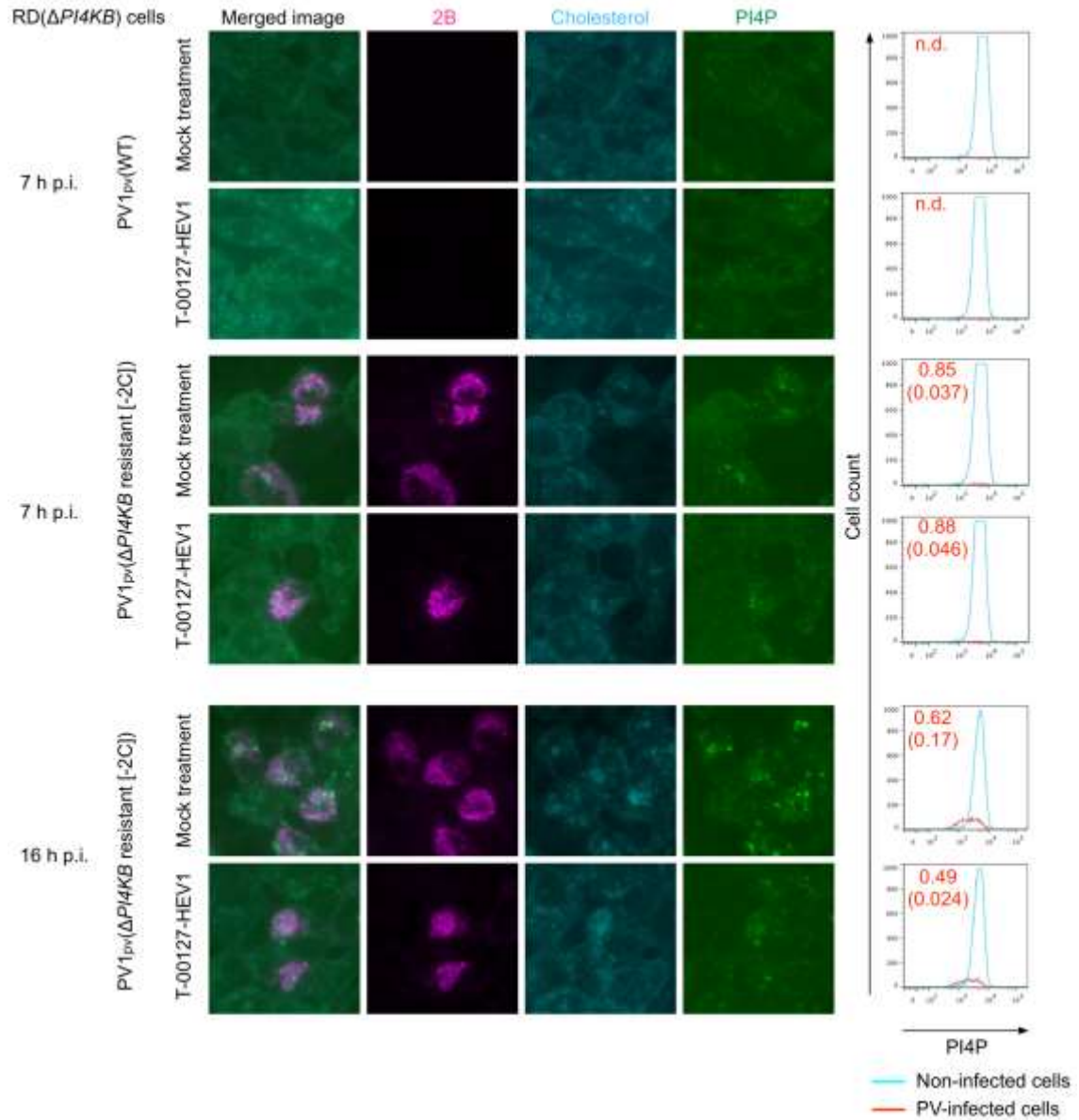


Figure S8. Quantification of PI4P and cholesterol in infected RD(Δ PI4KB) cells.

Left panels: Localization of 2B, cholesterol, PI4P in RD(Δ PI4KB) cells infected with PV1_{pv}(WT) at 7 h p.i. or with PV1_{pv}(Δ PI4KB resistant [-2C]) at 7 or 16 h p.i. at an MOI of 2.5 in the absence or presence of T-00127-HEV1 (10 μ M). Cyan, filipin III (staining of unesterified cholesterol); green, PI4P; magenta, 2B.

Right panels: Flow cytometry analysis of RD(Δ PI4KB) cells infected with PV1_{pv}(WT) or PV1_{pv}(Δ PI4KB resistant [-2C]) at an MOI of 1.0 in the absence or presence of T-00127-HEV1 (10 μ M) at indicated time with anti-2B and anti-PI4P antibodies. Ratios of geometric means of PI4P signals in the PV1_{pv}-infected cells to non-infected cells are determined with standard deviation (in parentheses) in the right graphs. n.d.; not detectable. $n = 3$.

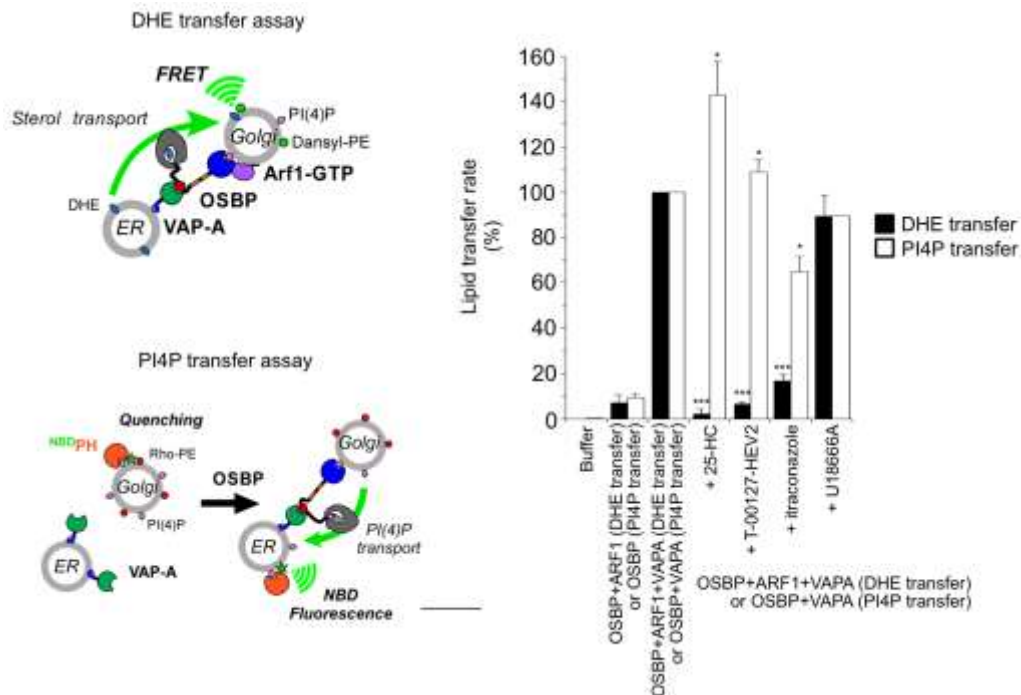


Figure S9. Effects of T-00127-HEV2 on lipid transfer activities of OSBP.

In vitro transfer of a cholesterol analog DHE or PI4P by OSBP in the presence of indicated compounds (1 μ M) were analyzed. Itraconazole (OSBP inhibitor) and U18666A (NPC1 inhibitor) were used as positive and negative control of the assays, respectively. Schematic views of the assays and the lipid transfer rates (%) are shown. $n = 3$ (DHE transfer assay) or 2 (PI4P transfer assay).

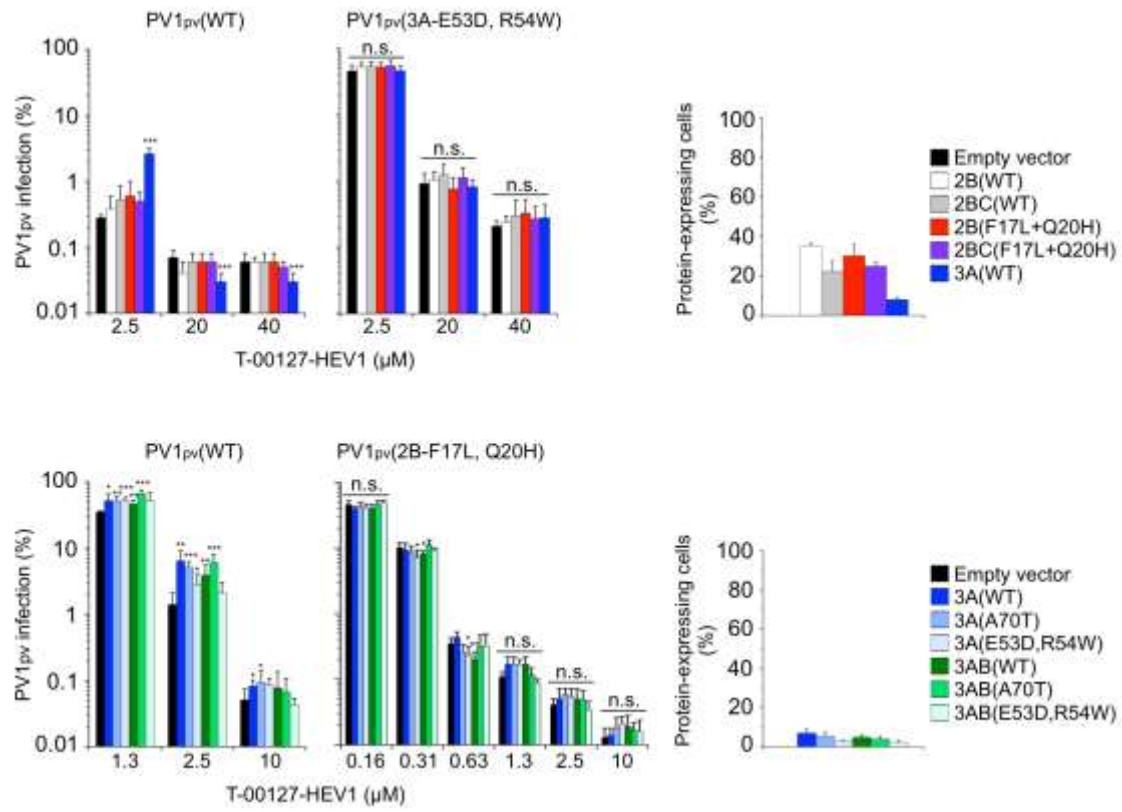


Figure S10. *Trans*-complementation with viral proteins.

HEK293 cells expressing each viral protein were infected with PV1_{pv} at an MOI of 0.1 in the presence of indicated concentrations of T-00127-HEV1. PV1_{pv} infection in the absence of T-00127-HEV1 is taken as 100%. Population of viral protein-expressing cells (%) is shown. $n = 3$.

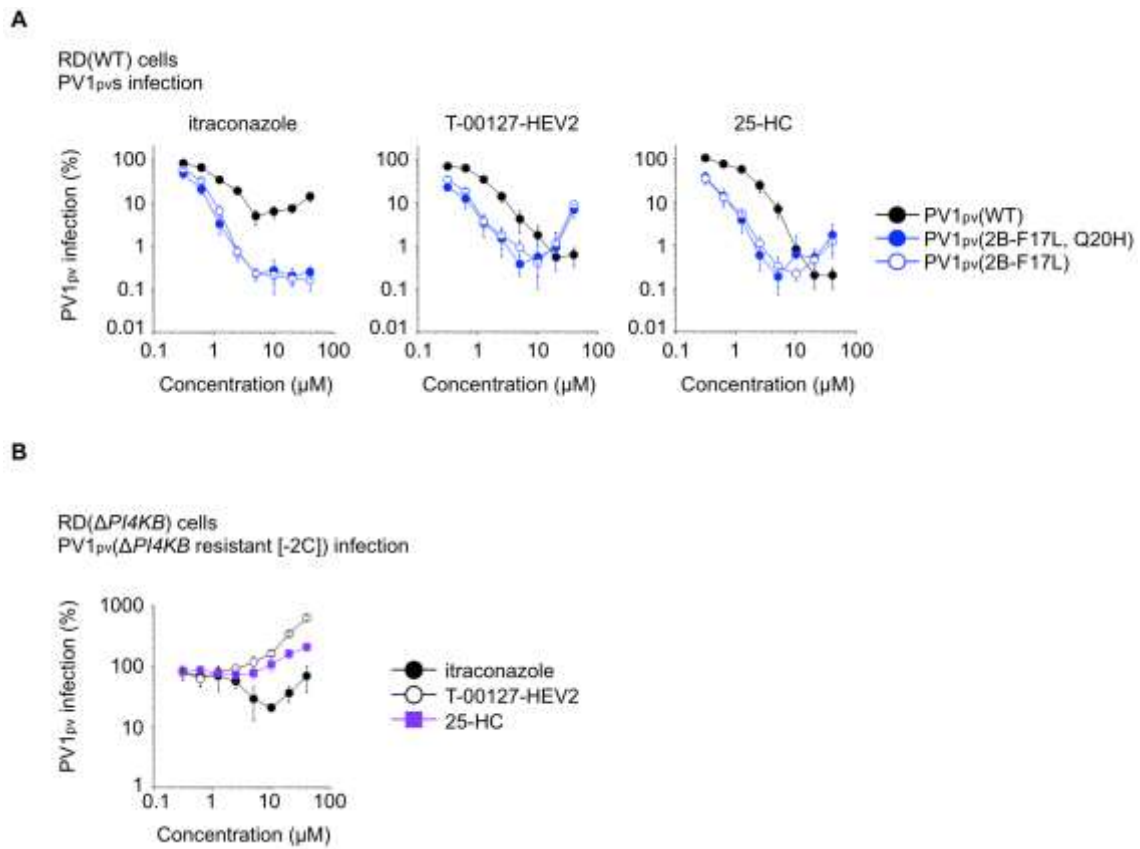


Figure S11. Effect of OSBP inhibitors on PV1_{pv} infection.

(A) Inhibitory effects of OSBP inhibitors on the infection of PV1_{pv} mutants in RD(WT) cells.

(B) Inhibitory effects of OSBP inhibitors on the infection of PV1_{pv} (Δ PI4KB resistant [-2C]) mutant in RD(Δ PI4KB) cells. PV1_{pv} infection in the absence of compounds is taken as 100%. $n = 3$.

Methods for supporting information

Cells. RD cells (human rhabdomyosarcoma cell line) and HEK293 cells (human embryonic kidney cells) were cultured as monolayers in Dulbecco's modified Eagle medium (DMEM) supplemented with 10% fetal calf serum (FCS). A *PI4KB*-knockout RD cell line was generated using a Clustered Regularly Interspaced Short Palindromic Repeats (CRISPR)/Cas9 GeCKO v2.0 system (a gift from Feng Zhang, Addgene, 1000000048)¹. RD cells were transfected with a lentiCRISPRv2 plasmid encoding a targeting sequence for *PI4KB* gene (5'-ATAAGCTCCCTGCCCCGAGTC-3') in the single-guide-RNA-coding region using a lipofectamine 3000 reagent (Invitrogen). A *PI4KB*-knockout cell line (RD[Δ *PI4KB*]) was obtained by subcloning of the transfected cells after selection with PV1(Sabin) infection.

Viruses. PV1(Sabin) is derived from a stock in NIID. Encephalomyocarditis virus (EMCV) was a kind gift from Kazuya Shirato (Department of Virology III, National Institute of Infectious Diseases, Japan). Luciferase-encoding Sendai virus (SeV-luc) was a kind gift from Atsushi Kato (Division of Quality Assurance, National Institute of Infectious Diseases, Japan). Wild-type type 1 PV pseudovirus (PV1_{pv}[WT]), which encapsidated luciferase-encoding PV replicon with the capsid protein of Mahoney strain, was used for evaluating infectivity. The G5318A(3A-A70T) mutation (enviroxime resistant) and newly identified mutations were introduced to PV1_{pv}. A PV1_{pv} mutant (139[+25aa]), which has a short open reading frame before the initiation codon causing reduced protein synthesis (17% of WT) and shows delayed replication kinetics², was used as a control in this study.

Plasmids. Expression vectors for N-terminally FLAG-tagged *PI4KB* mutants (GenBank: NM_001198773, UniProt: Q9UBF8-2) were constructed with pTK-Gluc vector (NEW ENGLAND BioLabs)³. Expression vectors for N-terminally EGFP-tagged PV 2BC3ABCD polyprotein were constructed with pHEK293 Ultra Expression Vector I (Takara Bio).

Compounds. A specific *PI4KB* inhibitor, T-00127-HEV1, was supplied by Pharmeks (P2001S-271690, purity >99%, determined by liquid chromatography-mass spectrometry [LC-MS])⁴. An OSBP inhibitor, T-00127-HEV2⁵, was kindly provided from Hirotatsu Kojima (Drug Discovery Initiative, The University of Tokyo) (purity >99%, determined by LC-MS). The 23-(dipyrrometheneboron difluoride)-24-norcholesterol (BODIPY-cholesterol) was purchased from Avanti Polar Lipids (810255P).

Antibodies. The primary antibodies below are used at the indicated dilutions for the indicated methods: rabbit anti-PV 2B antibody (raised with peptides WLRKKACDVLEIPYVIKQ, corresponding to amino acids 80 to 97 of PV 2B protein) (1:2000, immunocytochemistry and flow cytometry), rabbit anti-PV 3A antibody (raised with peptides DLLQAVDSQEVVDY, corresponding to amino acids 23 to 36 of PV 3A protein) (1:20, Western blot), rabbit anti-PV 3D antibody (raised with peptides GEIQWMRPSKEVGYPIINA, corresponding to amino acids 1 to 19 of PV 3D protein)

(1:250, Western blot)⁶, mouse anti-GM130 antibody (BD Biosciences, 610822, mouse IgG1) (1:100, immunocytochemistry), rabbit anti-PI4KB antibody (Merck Millipore, 06-578, rabbit IgG)(1:100, immunocytochemistry), mouse anti-PI4KB antibody (BD Biosciences, 611816, mouse IgG2a)(1:1000, Western blot), mouse anti-PI4P antibody (Echelon Biosciences, Z-P004, mouse IgM)(1:500, flow cytometry). Rabbit anti-PV 2C antibody (1:500, Western blot) was a kind gift from Tomoichiro Oka (Department of Virology II, National Institute of Infectious Diseases, Japan).

Secondary antibodies below were used in this study at the indicated dilutions for the indicated methods: goat anti-rabbit IgG antibodies conjugated with Alexa Fluor Plus 488, Alexa 594, or Alexa 647 (Thermo Fisher Scientific, A32731, A11037, or A21245, respectively)(1:1000, immunocytochemistry and flow cytometry), and goat anti-mouse IgG antibodies conjugated with Alexa Fluor Plus 488 (Thermo Fisher Scientific, A32723)(1:1000, immunocytochemistry), anti-mouse IgM antibody conjugated with Alexa 488 (Thermo Fisher Scientific, A21042)(1:1000, flow cytometry), goat anti-rabbit or anti-mouse IgG antibodies conjugated with horseradish peroxidase (Thermo Fisher Scientific, 32460 or 32430) (1:200, Western blot). Hoechst 33342 (1:2000, immunocytochemistry) (Molecular Probes) was used for counterstaining of nuclei.

Measurement of anti-PV activities of PI4KB/OSBP inhibitors. RD(WT) cells or RD(Δ PI4KB) cells (7×10^3 cells per well in 20 μ L medium) in 384-well plates (Greiner Bio-One, 781080) were inoculated with 10 μ L of PV1_{pv} (800 infectious units [IU]) and 10 μ L of compound solution. Cells were incubated at 37°C for 7 or 16 h. Luciferase activity in the infected cells was measured with the Steady-Glo luciferase assay system (Promega) using a 2030 ARVO X luminometer (PerkinElmer).

Immunofluorescence. Cells were fixed with 3% paraformaldehyde for 10 min at room temperature, then permeabilized with 20 μ M digitonin in HBS (21 mM HEPES buffer [pH 7.4], 1.8 mM disodium hydrogen phosphate, 137 mM NaCl, 4.8 mM KCl) for 5 min at room temperature. Cells were washed with HBS and stained with primary antibodies for 30 min at 37°C. Cells were washed with HBS and stained with secondary antibodies with or without Hoechst 33342 for 20 min at 37°C.

Viral RNA synthesis was visualized using a Click-iT RNA Imaging Kit (cat#: C10330, Invitrogen). RD(WT) cells (4×10^4 cells/well) were pre-labeled with 5 μ M BODIPY-cholesterol at 37°C for 24 h. Cells were infected with PV1_{pv}(WT) at an MOI of 2.5. At 3 h p.i., actinomycin D (final concentration, 0.01 mg/mL) and 5-ethynyl uridine (final concentration, 1 mM) were added to cells. At 5 h p.i., cells were collected and stained by Alexa Fluor 594 azide (nascent RNA) and anti-2B antibody according to the instructions from the manufacturer. Maximum projection images of cells were reconstructed from confocal images obtained at intervals of 0.2 μ m along the optical z-axis (1.4- to 1.8- μ m thickness; total number of confocal sections, 70 to 90) using a DSU spinning disk confocal microscopy (Olympus) with MetaMorph software (Molecular Devices, LLC.).

Trans-complementation with PI4KB mutants. RD(Δ PI4KB) cells (2.2×10^4 cells)

were transfected with the expression vectors for N-FLAG-PI4KB mutants. At 24 h post-transfection (p.t.), cells were infected with 20,000 IU of PV1_{pv}, then incubated at 37°C for 7 h for the measurement of luciferase activity.

Trans-complementation with viral proteins. HEK293 cells (1.2×10^4 cells per well in 20 μ L medium) in 384-well plates (Greiner Bio-One, 781080) were transfected with viral proteins expression vectors (0.02 μ g) using a TransIT-PRO Transfection Kit (Mirus, MIR5700). At 24 h p.t., cells were infected with PV1_{pv} at an MOI of 0.1 in the presence of T-00127-HEV1. Luciferase activity in the infected cell was measured at 7 h p.i.

Development of RO in replication-incompetent system. RD(WT) cells or RD(Δ PI4KB) cells (6×10^5 cells/well) were plated into a 96-well glass bottom SensiPlate (Greiner Bio-One, 655896). Cells were transfected with 200 ng of EGFP-2BC3ABCD expression vectors. At 24 h p.t., cells were fixed and stained for 2B as a marker of the RO with rabbit anti-2B antibody and goat anti-rabbit IgG antibody conjugated with Alexa Fluor 568 (Thermo Fischer Scientific, A11036). Images were collected at 20 \times magnification using a BZ-9000 fluorescence microscopy (Keyence). The number of cells with the RO in a wide perinuclear area observed in PV-infected cells (normal-sized RO) or with the RO in a small area observed in RD(Δ PI4KB) cells (small RO) were counted using CellProfiler software ⁷. Cells with the normal-sized RO (median typical diameter, 23 pixels) or with the small RO (median typical diameter, 12 pixels) were detected in a typical diameter range of 16 to 40 pixels or 10 to 15 pixels, respectively.

Measurement of luciferase signals per infected cell. RD(WT) cells or RD(Δ PI4KB) cells (1.1×10^4 cells per well in 20 μ L medium) were cultured in two 384-well plates; one for luciferase assay (Greiner Bio-One, 781080) and the other for counting of infected cells (Greiner Bio-One, 781090). The cells were inoculated with 10 μ L of PV1_{pv} (about 400 infectious units [IU]), and then incubated at 37°C for 7 or 16 h. Luciferase activity in the infected cells was measured with the Steady-Glo luciferase assay system (Promega) using a 2030 ARVO X luminometer (PerkinElmer). The numbers of infected cells in one well of the plates were determined by indirect immunofluorescence for 2B. Images were collected at 4 \times magnification using a BZ-9000 fluorescence microscopy (Keyence), and then analyzed by using CellProfiler software ⁷. The average RLU per infected cell was determined by dividing observed RLU per well by the number of infected cells per well.

Flow cytometry. HEK293 cells (8.0×10^5 cells) infected with PV1_{pv} at an MOI of 1 in the absence or presence of T-00127-HEV1 (10 μ M). Cells were collected at 7 h p.i. in 0.8 mL of 10%FCS-DMEM, then fixed with 3% paraformaldehyde for 10 min at room temperature, and permeabilized with 20 μ M digitonin in HBS for 5 min. Cells were incubated with anti-2B and PI4P antibodies for 30 min at 37°C. Cells were washed 2 times by 0.5% BSA in HBS, then incubated with secondary antibodies conjugated with Alexa Fluor 647 (for detection of anti-2B antibody) and Alexa Fluor 488 (for detection

of anti-PI4P antibody) dyes for 20 min at 37°C. Cells were suspended in 250 µL of HBS. About 5.0×10^4 cells were measured per sample with a BD FACSCanto™ II Flow Cytometer (BD Biosciences). Data were analyzed using FlowJo software (FLOWJO, LLC). Relative intensity of PI4P signals was determined as below:

$$\text{Relative intensity of PI4P signals} = \left(\frac{\text{PI4P signals in PV1pv} - \text{infected cells}}{\text{PI4P signals in non - infected cells}} \right)$$

Net amount of produced PI4P was determined as below:

$$\text{Net amount of produced PI4P} = \text{relative intensity of PI4P signals} - 1$$

***In vitro* DHE and PI4P transfer assay.** The method to measure the sterol and PI4P transfer activities of OSBP has been described previously⁸. Briefly, sterol transfer from ER-like liposomes (containing 18% DHE) to Golgi-like liposomes doped with dansyl-phosphatidylethanolamine (DNS-PE) was determined by fluorescence measurement as Förster resonance energy transfer (FRET) signal from DHE to DNS-PE upon excitation of DHE (310 (1.5) nm) and emission from DNS-PE (525(5) nm). PI4P-transfer from Golgi-like liposomes doped with rhodamine-PE (Rho-PE) and containing 2% PI4P, to ER-like liposomes (containing 2% Cholesterol) was detected via a fluorescent PI4P probe (NBD-PH[FAPP1] : PH domain of FAPP1 protein labeled with the fluorophore NBD). When bound to PI4P on the Rho-PE doped Golgi-like liposomes, NBD fluorescence(Ex : 460 (1) nm; Em 530 (5) nm) is quenched by the rhodamine, but unquenched when bound to the ER-like liposomes upon transfer of PI4P from the Golgi-like to the ER-like liposomes.^[SEP]

Lipids : Egg PC (L-α-phosphatidylcholine), liver PI (L-α-phosphatidylinositol), brain PS (L-α-phosphatidylserine), brain PI4P (L-α-phosphatidylinositol-4-phosphate), Dansyl (DNS)-PE (1,2-dioleoyl-*sn*-glycero-3-phosphoethanolamine-N-(5-dimethylamino-1-naphthalenesulfonyl)), Rhodamine (Rhod)-PE (1,2-dipalmitoyl-*sn*-glycero-3-phosphoethanolamine-N-(lissamine rhodamine B sulfonyl)), and DOGS-NTA-Ni2+ (1,2-dioleoyl-*sn*-glycero-3-[(N-(5-amino-1-carboxypentyl)iminodiacetic acid)succinyl]) were purchased from Avanti Polar Lipids. Cholesterol and dehydroergosterol (DHE) were obtained from Sigma Aldrich. The concentration of DHE in stock solution in methanol was determined by UV-spectroscopy using an extinction coefficient of 13,000 M-1.cm-1.^[SEP] ER-like liposomes for DHE transfer assay contain: egg PC/brain PS/DOGS-NTA-Ni2+ (93/5/2 mol%) supplemented with 18% DHE, and Golgi-like liposomes contain: egg PC/liver PE/brain PS/liver PI/DNS-PE (63.5/19/5/10/2.5 mol%). For PI4P transfer assay, ER like liposome composition was egg PC/brain PS/DOGS-NTA-Ni2+ (93/5/2 mol%) supplemented with 2% cholesterol and Golgi-like liposomes contain: egg PC/liver PE/brain PS/liver PI/brain PI4P/Rho-PE (63.5/19/5/8/2/2 mol%).^[SEP]

Proteins : Full-length OSBP, VAPA[8-212]His6, NBD-PH(FAPP1) and ARF1 were purified as described previously⁸.^[SEP]Experiments were performed in a Shimadzu RF-5301-PC spectrofluorimeter equipped with a cylindrical quartz cell (volume 600 µl) under continuous stirring and equilibrated at 37°C. For DHE transfer assays, Golgi-like liposomes (63.3 µM total lipids) were loaded with ARF1.GTP (0.3 µM) and incubated

with 1 μ M VAPA[8- 212]His6 in HKM buffer (Hepes 50mM, pH7.4, potassium acetate 120 mM, MgCl₂ 1mM) in the presence of 1 μ M compounds (stock solution 100X in DMSO), prior to the addition of ER-like liposomes (63.3 μ M total lipids and of OSBP (100 nM final concentration). Methyl- β -cyclodextrin (1 mM) was used to determine the maximal FRET signal due to full sterol equilibration between ER-like and Golgi-like liposomes. For PI4P transfer assay, Rhod-PE dopped Golgi-like liposomes (300 μ M total lipids) were incubated in HKM buffer with 250 nM NBD-PH(FAPP1), 3 μ M VAPA[8-212]His6 in the presence or absence of 1 μ M compounds (stock solution 100 \times in DMSO). ER-like liposomes (300 μ M lipid) and 100 nM OSBP were sequentially added. Maximal signal corresponding to PI4P equilibration between both types of liposomes was determined by mixing control ER- and Golgi-like liposomes, each containing 1% PI4P.

Western blot. Samples were subjected to e-PAGEL 5-20% gradient polyacrylamide gel electrophoresis (Atto Corporation) in a Laemmli buffer system. Proteins in the gel were transferred to a polyvinylidene difluoride filter (Millipore, Immobilon) and blocked in iBindTM solution (Thermo Fischer Scientific). Filters were incubated with primary antibodies (anti-viral proteins antibodies), then with secondary antibodies (goat anti-rabbit or anti-mouse IgG antibodies conjugated with horseradish peroxidase [PIERCE], 1:200) in iBindTM Western System (Thermo Fischer Scientific). Signals were detected with SuperSignal West Femto Maximum Sensitivity Substrate (PIERCE), then analyzed with LAS3000 (FUJIFILM).

Reference

- 1 Sanjana, N. E., Shalem, O. & Zhang, F. Improved vectors and genome-wide libraries for CRISPR screening. *Nat Methods* **11**, 783-784, doi:10.1038/nmeth.3047 (2014).
- 2 Arita, M., Shimizu, H. & Miyamura, T. Characterization of in vitro and in vivo phenotypes of poliovirus type 1 mutants with reduced viral protein synthesis activity. *J. Gen. Virol.* **85**, 1933-1944 (2004).
- 3 Arita, M., Dobrikov, G., Purstinger, G. & Galabov, A. S. Allosteric Regulation of Phosphatidylinositol 4-Kinase III Beta by an Antipicornavirus Compound MDL-860. *ACS Infect. Dis.* **3**, 585-594, doi:10.1021/acsinfecdis.7b00053 (2017).
- 4 Arita, M. *et al.* Phosphatidylinositol 4-kinase III beta is a target of enviroxime-like compounds for antipoliovirus activity. *J. Virol.* **85**, 2364-2372, doi:10.1128/JVI.02249-10 (2011).
- 5 Arita, M. *et al.* Oxysterol-binding protein family I is the target of minor enviroxime-like compounds. *J. Virol.* **87**, 4252-4260, doi:10.1128/JVI.03546-12 (2013).
- 6 Arita, M. Phosphatidylinositol-4 kinase III beta and oxysterol-binding protein accumulate unesterified cholesterol on poliovirus-induced membrane structure. *Microbiol. Immunol.* **58**, 239-256, doi:10.1111/1348-0421.12144 (2014).
- 7 Kamentsky, L. *et al.* Improved structure, function and compatibility for CellProfiler: modular high-throughput image analysis software. *Bioinformatics* **27**, 1179-1180, doi:10.1093/bioinformatics/btr095 (2011).
- 8 Mesmin, B. *et al.* A Four-Step Cycle Driven by PI(4)P Hydrolysis Directs Sterol/PI(4)P Exchange by the ER-Golgi Tether OSBP. *Cell* **155**, 830-843, doi:10.1016/j.cell.2013.09.056 (2013).